

1 **Supplementary Data**

2
3 **CSN6 mediates nucleotide metabolism to promote tumor**
4 **development and chemoresistance in colorectal cancer**

5
6
7 Shaomin Zou^{1,2}, Baifu Qin^{1,2}, Ziqing Yang^{1,2}, Wencong Wang^{1,2}, Jieping Zhang^{1,2},
8 Yijing Zhang^{1,2}, Manqi Meng^{1,2}, Junyan Feng^{1,2}, Yunling Xie^{1,2}, Ling Fang³, Lishi
9 Xiao^{1,2}, Peng Zhang^{1,2}, Xiangqi Meng^{1,2}, Hyun Ho Choi^{1,2}, Weijie Wen^{1,2}, Qihao Pan^{1,2},
10 Bart Ghesquière⁴, Ping Lan^{1,2,5#}, Mong-Hong Lee^{1,2#}, and Lekun Fang^{1,2,5#}

11
12
13
14
15
16
17
18 This file contains:

19 - Supplementary Materials and Methods

20 - Supplementary Figure S1-S11

21
22
23
24
25
26
27
28
29
30

31 **Supplementary Materials and Methods**

32 **Patient-derived organoid (PDO)**

33 Fresh human CRC tumor tissues were collected and cut into pieces, then washed
34 with ice-cold PBS, digested with EDTA. Matrigel polymerization for 10 min at 37°C.
35 Then, organoids were cultured with advanced DMEM/F12 supplemented with 2mM
36 GlutaMAX, penicillin/streptomycin, $1 \times$ B27, 10 mM HEPES, 10 nM gastrin I
37 (Biogems), $1 \times$ N2 (Life Technologies), 1mM N-acetylcysteine (Sigma), 500 nM A83-
38 01 (Biogems), 50 ng/mL recombinant EGF, 100 ng/ mL recombinant Noggin
39 (Peprotech), 10mM nicotinamide (Sigma), 500ng/mL R-spondin-1(Peprotech), 10 μ M
40 Y-27632 (Abmole) and 10 μ M SB202190 (Sigma). After seeding, organoids were
41 treated with shRNA virus or control for 12h. Removed the virus and added the new
42 culture medium with nucleosides supplementation. Organoid diameters were calculated
43 by Image J (RRID: SCR_003070).

44

45 **Immunoblot and Immunoprecipitation**

46 Total cells lysates for immunoblotting or immunoprecipitation were lysed with
47 buffer (0.1%Triton-100, 50 mM Tris-Cl, pH 7.5, 0.1% NP-40, 150 mM NaCl, 0.1 M
48 EDTA) supplemented with a cocktail of phosphate and proteinase inhibitors for 30
49 minutes at 4°C. For immunoblot, samples were separated by SDS–PAGE. Antibodies
50 specific for CSN6 (Enzo Life Sciences Cat# BML-PW8295, RRID: AB_10539117),
51 DDX5 (Cell Signaling Technology, #9877), β -Trecp (Cell Signaling Technology,
52 #4394S), Flag-Tag (Sigma, F1804), HA-Tag (Cell Signaling Technology, #3724S),

53 Myc-Tag (Cell Signaling Technology, #2276S), PHGDH (Sigma, HPA021241), and
54 GAPDH (Proteintech, 10494-1-AP) were purchased from the indicated companies. For
55 immunoprecipitation, cell lysates were prepared as before and rotated 1mg proteins
56 with antibody at 4°C overnight, then immunoprecipitated by Protein A/G beads; or
57 incubated cell lysates with anti-Flag or anti-myc beads at 4°C overnight. The
58 immunoprecipitates and input were subjected to western blot analysis.

59

60 **Tissue microarray assay**

61 For tissue microarray, we performed immunohistochemistry (IHC) on 267
62 paraffin-embedded samples obtained from the First Affiliated Hospital of Sun Yat-sen
63 University. Then the original immunohistochemistry slides were scanned and captured
64 images by Aperio Versa (Leica Biosystems). Subsequently, H-score was calculated by
65 the Aperio Versa base on the staining intensity and percentage of positive stained tumor
66 cells. The cut-off point was defined based on the receiver operating characteristic curve.
67 Spearman correlation analysis or Chi-square test was used to estimate the association
68 between CSN6, DDX5 and PHGDH staining intensities.

69

70 **Immunohistochemistry**

71 Immunohistochemical staining was performed on 5- μ m paraffin sections prepared
72 from tumor tissues. Briefly, sections were deparaffinized in xylene, hydrated in graded
73 ethanol, then immersed in 3% hydrogen peroxide to quench for endogenous peroxidase
74 and probed with primary antibody against CSN6 (1:500, Enzo Life Sciences Cat#
75 BML-PW8295, RRID: AB_10539117), DDX5 (1:4000, Abcam, ab21696) or PHGDH

76 (1:1000, Sigma, HPA021241), Ki67 (1:500, Cell Signaling Technology, #9449) at 4°C
77 overnight. Subsequently, immunostaining was visualized with diaminobenzidine and
78 slices were counterstained with hematoxylin.

79

80 **Cell proliferation assay**

81 The incucyte live cell analysis system (Essen Bioscience) is performed for
82 detecting cell proliferation. Cells were seeded in 12-well plates and put inside
83 incubators, then machine would automatically obtain and analyze images during the
84 progress of an experiment while cells remain unperturbed. The cell counting kit-8
85 (CCK8) assay was also used to examine cell viability. Cells (3000/well) were seeded
86 in 96-well plates and were incubated for 24, 48, or 72 hours. Subsequently, 10 μ L of
87 CCK8 (APExBIO) solution was added to each well and incubated for 3 h, then the
88 absorbance value (OD) was measured at 450 nm. Data represent the means \pm SD. of
89 three independent experiments.

90

91 **Colony formation assay**

92 Cells were seeded into 6-well plates (800 cells per well) and then cultured for 10-
93 14 days. Culture mediums were refreshed every 3 days. After visible colonies formed,
94 cells were fixed with 4% paraformaldehyde (PFA) and stained with crystal violet.
95 Finally, the number of colonies were counted by image J.

96

97

98

99 **DESI-MS imaging**

100 Imaging experiments were carried out on a 2D DESI system (Prosolia,
101 Indianapolis, USA) mounted on a Xevo-G2-XS quadrupole-time of flight (Q-TOF)
102 (Waters Corporation, Wilmslow, UK). The solvent spray consisted of 95% methanol
103 and 5% water. Spray conditions used were a flow rate of 2 μ l/minutes (using a syringe
104 pump from Harvard Apparatus, Inc., Holliston, MA), with a nebulising gas of nitrogen
105 at 4 bar pressure. Typical positions of the sprayer were used (sprayer 1.5mm above
106 surface, 6mm sprayer to capillary distance, 75° sprayer impact angle, 5° collection
107 capillary angle). The source temperature was 100 °C and the capillary voltage was set
108 between 4.82 and 5kV. Images were acquired using a scan rate of 1-10 scans/second,
109 and a mass range of 50-1200 Da. The spatial resolution varied from 40-200 μ m. Images
110 were processed and normalised to total ion current (TIC) using the High-Definition
111 Imaging (HDI) v1.4 (Waters, Wilmslow, UK). MS/MS experiments were carried out
112 on a Xevo-G2-XS Q-TOF mass spectrometer using argon as the collision gas and a
113 collision energy range of 20 V - 40 V. Spray conditions were the same as DESI imaging.
114

115 **Real Time qPCR**

116 Total RNA was isolated with TRIZOL reagent (Invitrogen) and reverse
117 transcription was performed by ReverTra Ace® qPCR RT Master Mix with gDNA
118 Remover (TOYOBO), according to the manufacturer's protocol. Then the gene
119 expression was quantified dependent on the LightCycler480 PCR system (Roche) by
120 using 2 \times SYBR Green qPCR Master Mix (biotool, #B21203). All the target genes were

121 normalized to GAPDH. Primer sequences were listed as follows: *CSN6* F:
122 TCATCGAGAGCCCCCTCTTT; *CSN6* R: CCAATGCGTTCCGCTTCCT; *DDX5* F:
123 GCCGGGACCGAGGGTTTGGT; *DDX5* R: CTTGTGCTGTGCGCCTAGCCA;
124 *PHGDH* F: CTGCGGAAAGTGCTCATCAGT; *PHGDH* R:
125 TGGCAGAGCGAACAATAAGGC; *GAPDH*F: GGAGCGAGATCCCTCCAAAAT;
126 *GAPDH*R: GGCTGTTGTCATACTTCTCATGG.

127

128 **Exogenous RNA pull-down assays**

129 For exogenous RNA pull-down assay, RNAs were *in vitro* transcribed
130 using Thermo Scientific Transcript Aid T7 High Yield Transcription Kit (Thermo,
131 #K0441) according to the manufacturer's instructions. Next, the Thermo Scientific
132 Pierce RNA 3' End Desthiobiotinylation Kit uses T4 RNA ligase to attach a single
133 biotinylated nucleotide to the 3' terminuses of an RNA strand (Thermo, #20163). Cell
134 lysates were prepared using standard lysis buffer, binding of Labeled RNA to
135 Streptavidin Magnetic Beads, then binding RNA-Binding Proteins, incubate 30-60
136 minutes at 4°C with agitation or rotation. Washing and elution of RNA-Binding Protein
137 complexes, finally RNA-interactive proteins were detected by WB analysis.

138

139 **mRNA stability analysis**

140 DLD1 cells were treated with *DDX5* shRNA or scramble, then incubated with
141 Actinomycin D (10mg/mL) for 0, 1, 2 or 4h. Following RNA isolation with Trizol and
142 quantification with qPCR.

143 **Turnover assay**

144 Cells were infected with virus carried shRNA or transfected with indicated
145 plasmids, then cycloheximide was added into the media at a final concentration of 100
146 $\mu\text{g/ml}$. Harvested cells at the indicated time points after cycloheximide treatment, and
147 analyzed protein levels by immunoblotting.

148

149 **Ubiquitination assay**

150 HCT116 and HEK293T cells were co-transfected with the indicated plasmids for
151 48 h and treated with MG132 for an additional 6 h. The cell lysates were incubated with
152 Ni-NTA agarose beads to pull down proteins conjugated to His-ubiquitin, then washed,
153 and analyzed by western blotting with indicated antibody.

154

155

156

157

158

159

160

161

162

163

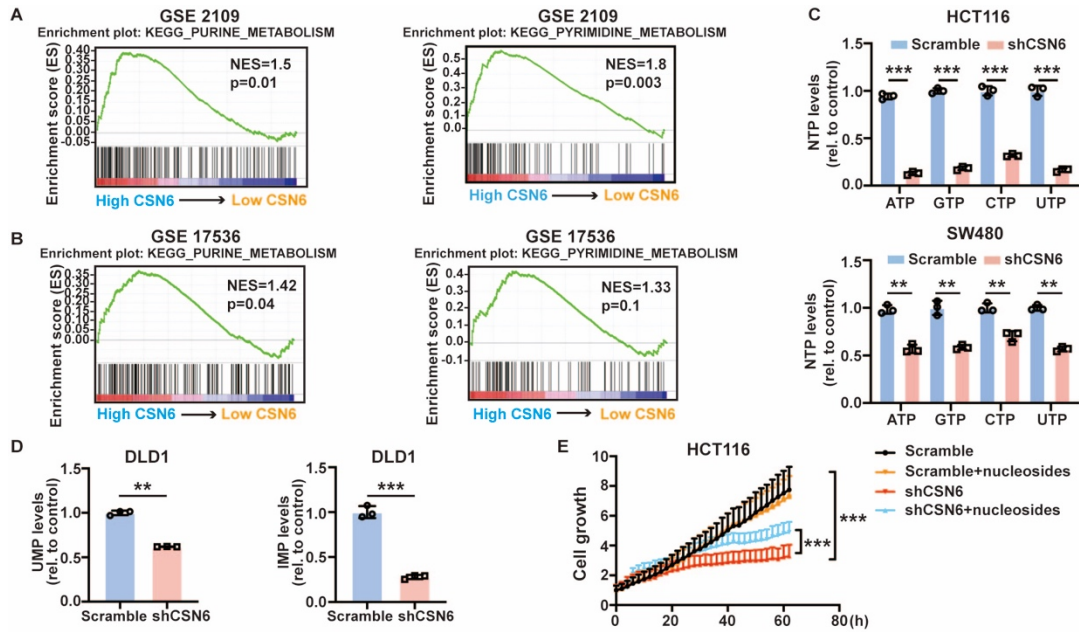
164

165

166

167

168



169

170 **Supplementary Fig.S1**

171 Depletion of CSN6 decreased nucleotide synthesis. **A, B**, An enrichment analysis of
 172 gene sets available from the CRC database GSE2109 and GSE17536 revealed that
 173 CSN6 expression is positively correlated with pyrimidine and purine metabolism. **C**,
 174 NTPs (ATP, GTP, UTP, CTP) levels in HCT116 and SW480 cells with or without
 175 CSN6 shRNA treatment. The data are presented as the means \pm SD. ** $p < 0.01$,
 176 *** $p < 0.001$, t test. **D**, UMP and IMP levels in DLD1 cells stably expressing CSN6
 177 shRNA (n=3). The data are presented as the means \pm SD. ** $p < 0.01$, *** $p < 0.001$, t test.
 178 **E**, The effects of nucleosides repletion on rescuing shCSN6 inhibiting cell growth.
 179 *** $p < 0.001$, by the two-way ANOVA.

180

181

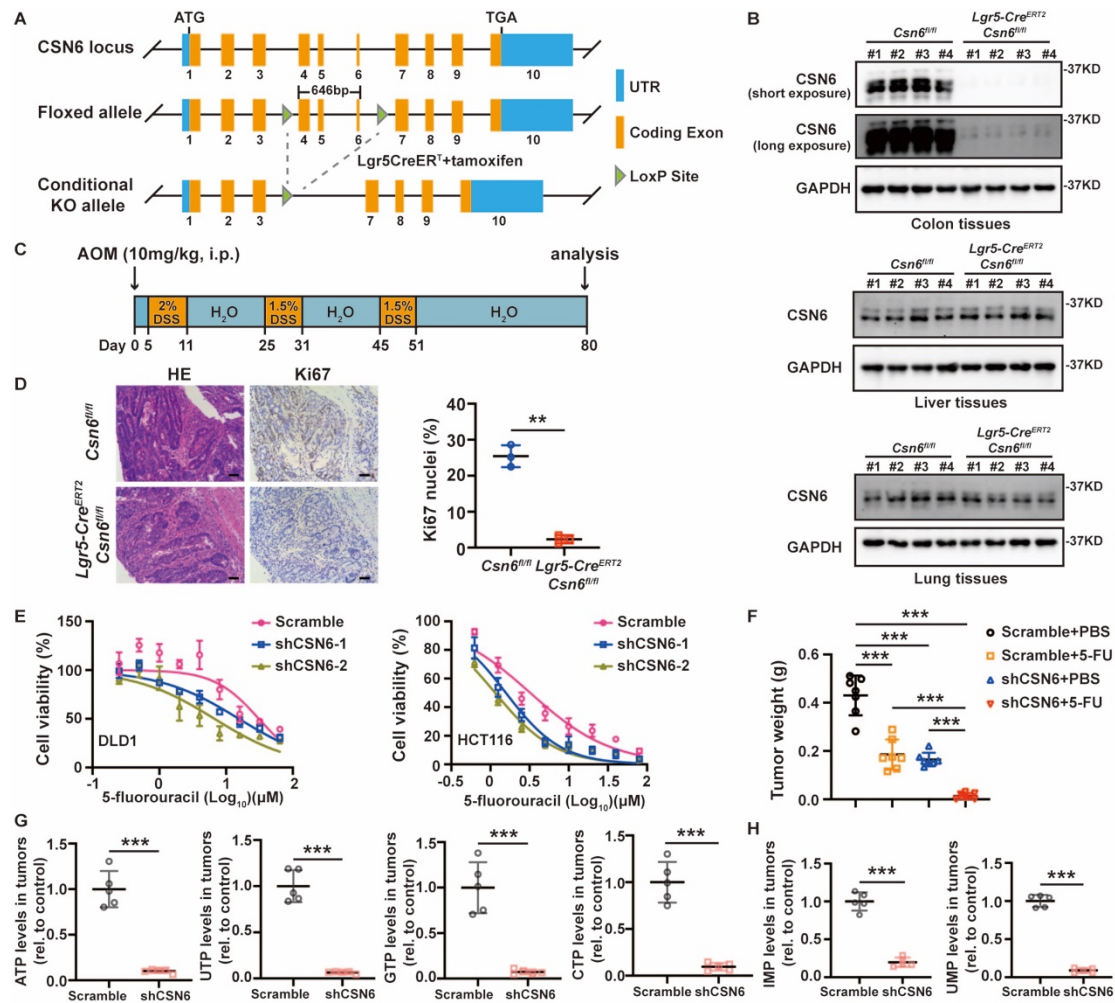
182

183

184

185

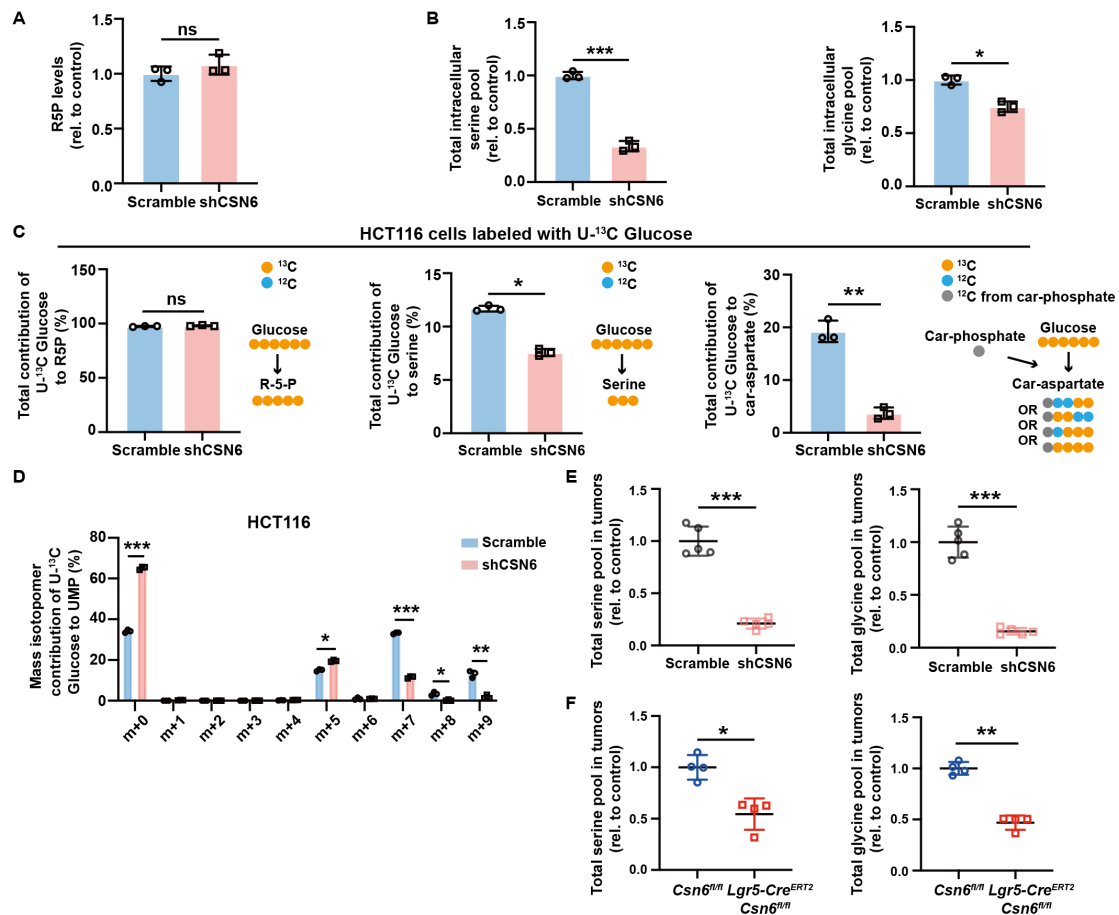
186



187

188 **Supplementary Fig.S2**

189 CSN6 promotes CRC progression and drug resistance. **A**, Overview of the CSN6
 190 conditional knockout (*Csn6^{CKO}*) mice targeting strategy. **B**, CSN6 expression in colon,
 191 liver and lung tissues from *Lgr5-Cre^{ERT2};Csn6^{fl/fl}* and *Csn6^{fl/fl}* mice were determined by
 192 western blot. **C**, Scheme of AOM/DSS model. **D**, H&E (hematoxylin and eosin)
 193 staining and Ki67 immunohistochemistry of colon tumor sections from *Lgr5-
 194 Cre^{ERT2};Csn6^{fl/fl}* and *Csn6^{fl/fl}* mice. Scale bar, 100µm. The data are presented as the
 195 means ± SD. **p<0.01. **E**, DLD1 and HCT116 cells were treated with 5-FU at different
 196 concentrations, and the cell viability was then evaluated using the CCK8 assay. The
 197 data are presented as the means ± SD. **F**, Tumor weight of different nude mice groups
 198 (scramble; scramble+5-FU; shCSN6; shCSN6+5-FU, n=7 for each group). The data are
 199 presented as the means ± SD. ***p<0.001 by One-Way ANOVA. **G**, NTPs (ATP, CTP,
 200 UTP, GTP) levels in control tumors (scramble) compared to CSN6 knockdown
 201 (shCSN6) DLD1 xenograft tumors (n=5 per group). The data are presented as the means
 202 ± SD. ***p<0.001, by non-parametric test. **H**, IMP and UMP levels in the control
 203 tumors (scramble) compared to CSN6 knockdown (shCSN6) DLD1 xenograft tumors
 204 (n=5 per group). The data are presented as the means ± SD. ***p<0.001, by non-
 205 parametric test.



206

207

Supplementary Fig.S3

208

Silencing of CSN6 impaired *de novo* nucleotide synthesis. **A**, Ribose-5-phosphate

209

levels in the control and shCSN6 expressing DLD1 cells. The data are presented as the

210

means \pm SD. ns: no significance, t-test. **B**, Intracellular serine and glycine levels in the

211

control and shCSN6 expressing DLD1 cells. The data are presented as the means \pm SD.

212

* $p < 0.05$, *** $p < 0.001$ by t-test. **C**, Incorporation of carbon atoms from [U-¹³C] glucose

213

into R5P, serine and car-aspartate in the control and shCSN6 expressing HCT116 cells.

214

The data are presented as the means \pm SD. * $p < 0.05$, ** $p < 0.01$, ns: no significance by

215

t-test. **D**, Fractional contribution of carbon atoms from [U-¹³C] glucose into the UMP

216

isotopomers (m+0 to m+9) in the control and shCSN6 expressing HCT116 cells. The

217

data are presented as the means \pm SD. * $p < 0.05$, ** $p < 0.01$, *** $p < 0.001$ by t-test. **E**,

218

Serine and glycine levels in the control and shCSN6 expressing DLD1 xenograft tumor

219

tissues (n = 5 per group). The data are presented as the means \pm SD. *** $p < 0.001$ by

220

non-parametric test. **F**, Serine and glycine levels in the colonic tumors from *Lgr5-*

221

Cre^{ERT2};Csn6^{fl/fl} and *Csn6^{fl/fl}* mice (n = 4 per group). The data are presented as the means

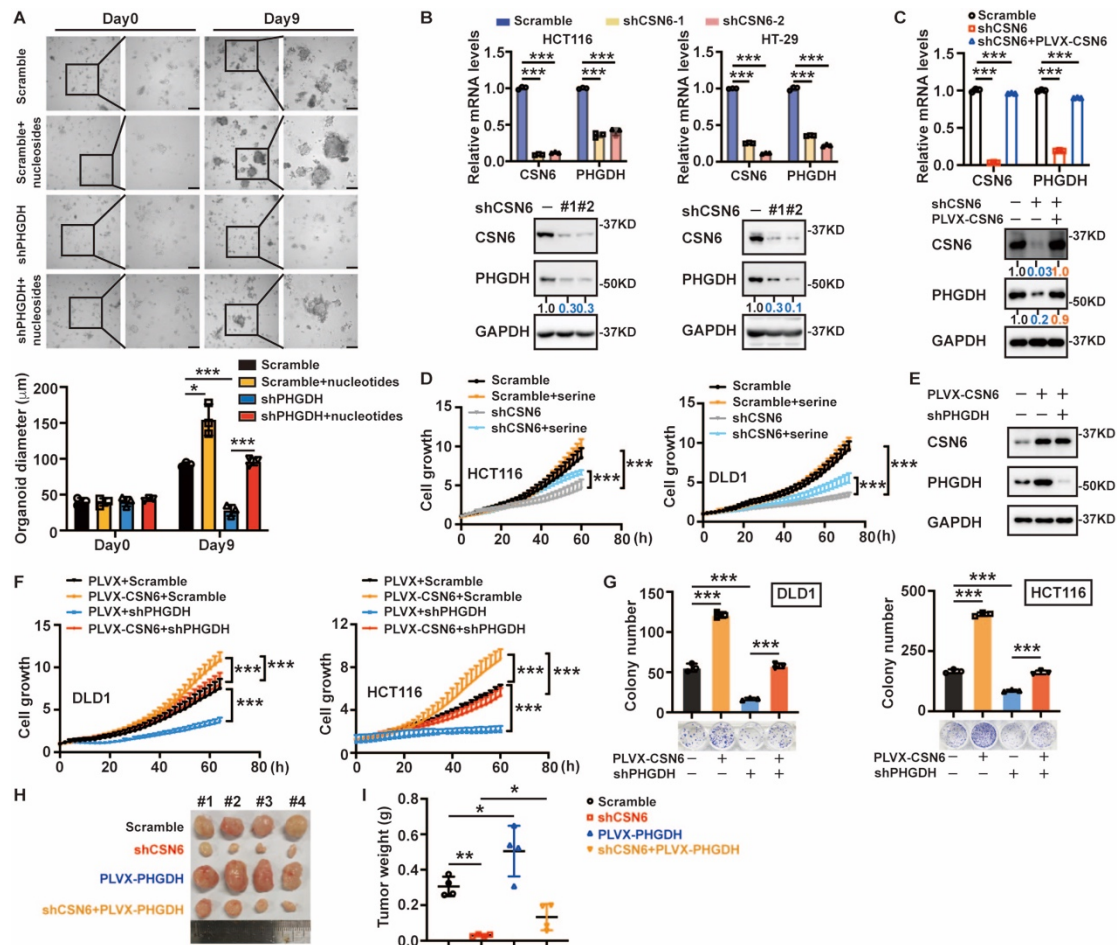
222

\pm SD. * $p < 0.05$, ** $p < 0.01$, by non-parametric test.

223

224

225



226

227

Supplementary Fig.S4

228 CSN6 promotes CRC progression in PHGDH-dependent manner. **A**, Nucleosides
 229 repletion (adenine, guanine, cytosine, uracil; 100 μ M) could rescue patient-derived
 230 tumor organoid (PDO) growth upon PHGDH depletion. The morphology of the
 231 organoids is shown. Scale bar: 100 μ m. Quantifications of organoid diameter are
 232 presented as the means \pm SD. * p <0.05, *** p <0.001. **B**, qRT-PCR and western blot
 233 analysis of PHGDH expression in HCT116 and HT-29 cells stably expressing CSN6
 234 shRNA or scramble. The data are presented as the means \pm SD. *** p <0.001 by One-
 235 Way ANOVA. **C**, DLD1 cells were infected with indicated virus. qRT-PCR and
 236 western blot were used to detected PHGDH expression. The data are presented as the
 237 means \pm SD. *** p <0.001 by the two-way ANOVA. **D**, Supplementation of serine
 238 rescued shCSN6 inhibited HCT116 and DLD1 cell growth. The data are presented as
 239 the means \pm SD. *** p <0.001 by the two-way ANOVA. **E**, Detection of CSN6 and
 240 PHGDH expression in control and PLVX-CSN6 DLD1 cells treated with shPHGDH.
 241 **F**, Proliferation assay of DLD1 and HCT116 cells with or without PLVX-CSN6 or
 242 shPHGDH treatment. The data are presented as the means \pm SD. *** p <0.001 by the
 243 two-way ANOVA. **G**, Effects of PHGDH depletion on the clonogenic ability of PLVX
 244 or PLVX-CSN6 DLD1 and HCT116 cells. Colony numbers were quantified. The data
 245 are presented as the means \pm SD. *** p <0.001. **H**, **I**, DLD1 cells with or without
 246 shCSN6 or PLVX-PHGDH infection were subcutaneously injected into nude mice

247 (n=4). The tumors were isolated at the end of the experiments. The tumor pictures (H),
248 and tumor weight (I) were shown.

249

250

251

252

253

254

255

256

257

258

259

260

261

262

263

264

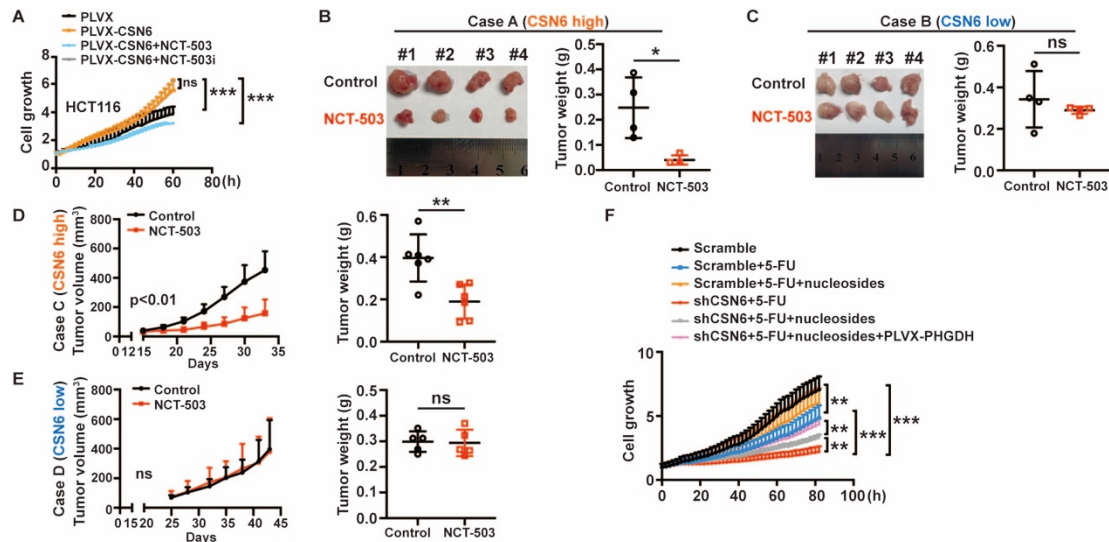
265

266

267

268

269



270

271 **Supplementary Fig.S5**

272 CSN6 promotes CRC tumorigenesis and chemoresistance through PHGDH. **A**,
 273 Proliferation assay of control and PLVX-CSN6 HCT116 cells treated with NCT-503 or
 274 NCT-503i. The data are presented as the means \pm SD. ***p<0.001 by the two-way
 275 ANOVA. **B**, Impact of NCT-503 on tumor growth and weight in mice bearing CSN6-
 276 high expressed PDXs (n=4 per group). The data are presented as the means \pm SD.
 277 *p<0.05 by non-parametric test. **C**, Impact of NCT-503 on tumor growth and weight in
 278 mice bearing CSN6-low expressed PDXs (n=4 per group). The data are presented as
 279 the means \pm SD. ns: no significance, by non-parametric test. **D**, Impact of NCT-503
 280 on tumor volume and weight in mice bearing CSN6-high expressed PDXs (Case C). The
 281 data are presented as the means \pm SD. **p<0.01 by non-parametric test. **E**, Impact of
 282 NCT-503 on tumor volume and weight in mice bearing CSN6-low expressed PDXs
 283 (Case D). The data are presented as the means \pm SD. ns: no significance, by non-
 284 parametric test. **F**, Incucyte machine was used to evaluate the effects of nucleosides
 285 repletion (adenine, guanine, cytosine, uracil; 100 μ M) on cancer cells proliferation upon
 286 CSN6 depletion, PHGDH overexpression and 5-FU treatment. The data are presented
 287 as the means \pm SD. **p<0.01; ***p<0.001 by the two-way ANOVA.

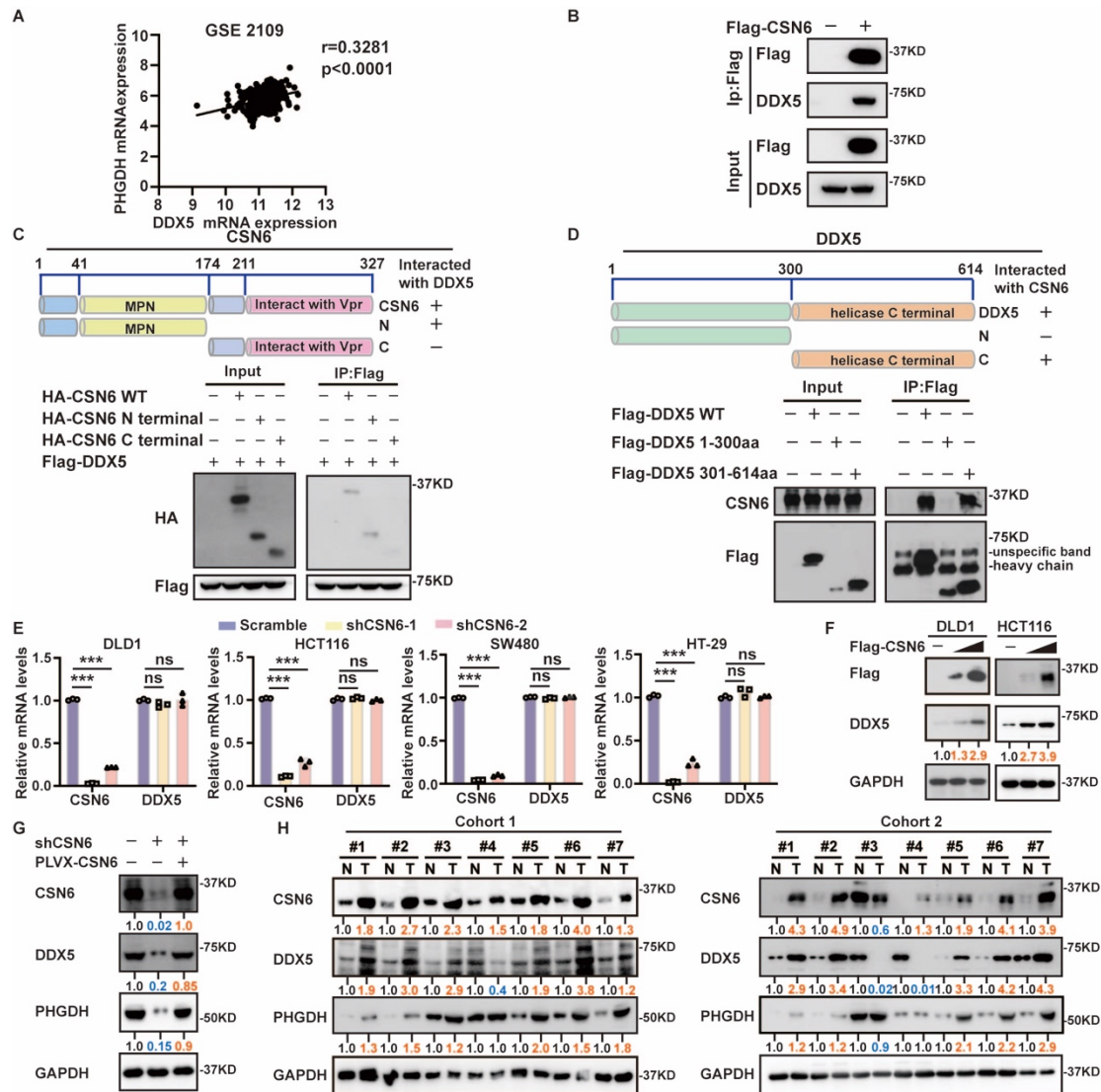
288

289

290

291

292



293

294

Supplementary Fig.S6

295

CSN6 interacts with DDX5 and regulates DDX5 protein expression. **A**, Pearson

296

correlation analysis of DDX5 and PHGDH in GEO: GSE2109. **B**, DLD1 cells were

297

transfected with Flag-CSN6 and vector. Cell lysates were then immunoprecipitated

298

with anti-Flag beads and immunoblotted with the indicated antibodies. **C**, Mapping of

299

CSN6-binding domains on DDX5. HEK293T cells were co-transfected with HA-CSN6

300

(aa 1-327), the N terminal of CSN6 (aa 1-174) or the C terminal of CSN6 (aa 175-327)

301

and Flag-DDX5. Cell lysates were immunoprecipitated with anti-Flag beads and

302

immunoblotted with anti-HA antibody. **D**, Mapping of DDX5-binding domains on

303

CSN6. HEK293T cells were transfected with Flag-DDX5 (aa 1-614), the N terminus

304

of DDX5 (aa 1-300) or the C terminus of DDX5 (aa 301-614). Cell lysates were

305

immunoprecipitated with anti-Flag beads and immunoblotted with anti-CSN6 antibody.

306

E, qRT-PCR analysis of DDX5 expression in control and shCSN6 expressing CRC

307

cells. The data are presented as the means \pm SD. *** $p<0.001$, ns: no significance, by

308

One-Way ANOVA. **F**, Western blot analysis of DDX5 expression in vector and CSN6

309

overexpressing CRC cells. **G**, DLD1 cells were infected with indicated virus. Western

310

blot was used to detected CSN6, DDX5 and PHGDH expression. **H**, Immunoblotting

311 analysis of CSN6, DDX5 and PHGDH protein levels in 14 pairs of CRC tumors (T)
312 and corresponding adjacent normal tissues (N).

313

314

315

316

317

318

319

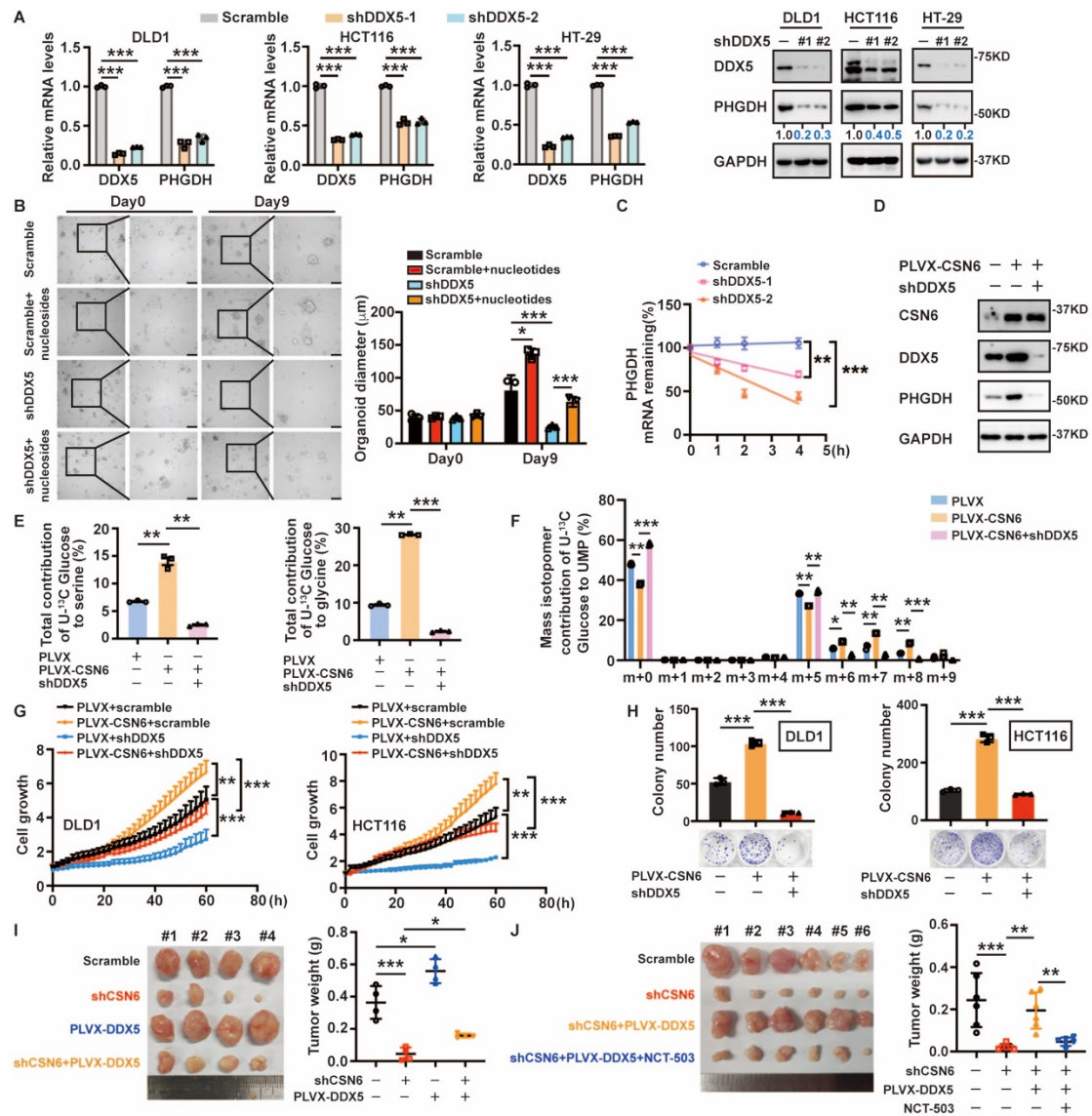
320

321

322

323

324



325

326 **Supplementary Fig.S7**

327 CSN6-DDX5-PHGDH axis promotes nucleotide biosynthesis and CRC progression. **A**,
 328 qRT-PCR and western blot analysis of PHGDH expression in control and shDDX5.
 329 expressing CRC cells. For the qRT-PCR, the data are presented as the means ± SD.
 330 ***p<0.001 by One-Way ANOVA. **B**, Nucleosides repletion could rescue patient-
 331 derived tumor organoid (PDO) growth upon DDX5 depletion. The morphology of the
 332 organoids is shown. Scale bar: 100 μm. Quantifications of organoid diameter are
 333 presented as the means ± SD. *p<0.05, ***p<0.001. **C**, Quantification of the half-life
 334 of PHGDH (% mRNA remaining) over time after actinomycin D (10 μg/ml) addition
 335 in DLD1 cells. Graph represents means ±SD. **p<0.01; ***p<0.001 by the two-way
 336 ANOVA test. **D**, Detection of CSN6, DDX5 and PHGDH expression in control and
 337 PLVX-CSN6 DLD1 cells treated with shDDX5. **E**, Incorporation of carbon atoms from
 338 [U-¹³C] glucose into serine, glycine in the cells with or without PLVX-CSN6 or
 339 shDDX5 treatment. The data are presented as the means ± SD. **p<0.01, ***p<0.001
 340 by One-Way ANOVA. **F**, Fractional contribution of carbon atoms from [U-¹³C]
 341 glucose into the UMP in the cells with or without PLVX-CSN6 or shDDX5 treatment.

342 The data are presented as the means \pm SD. * p <0.05, ** p <0.01, *** p <0.001 by One-
343 Way ANOVA. **G**, Cell proliferation of PLVX and PLVX-CSN6 DLD1 and HCT116
344 cells infected with scramble or shDDX5. Graph represents means \pm SD. ** p <0.01;
345 *** p <0.001 by the two-way ANOVA test. **H**, Effects of DDX5 depletion on the
346 clonogenic ability of PLVX-CSN6 DLD1 and HCT116 cells. Colony numbers were
347 quantified. The data are presented as the means \pm SD. *** p <0.001. **I**, DLD1 cells with
348 or without shCSN6 or PLVX-DDX5 infection were subcutaneously injected into nude
349 mice (n=4). The tumors were isolated at the end of the experiments. The tumor pictures
350 and tumor weight were shown. **J**, CSN6 knockdown through the injection of shRNA
351 lentivirus strongly inhibits the subcutaneous tumor growth of nude mice, which could
352 be rescued by stable overexpression of PLVX-DDX5. Furthermore, NCT-503
353 treatment could abrogate these effects. The tumor pictures and tumor weight were
354 shown.

355

356

357

358

359

360

361

362

363

364

365

366

367

368

369

370

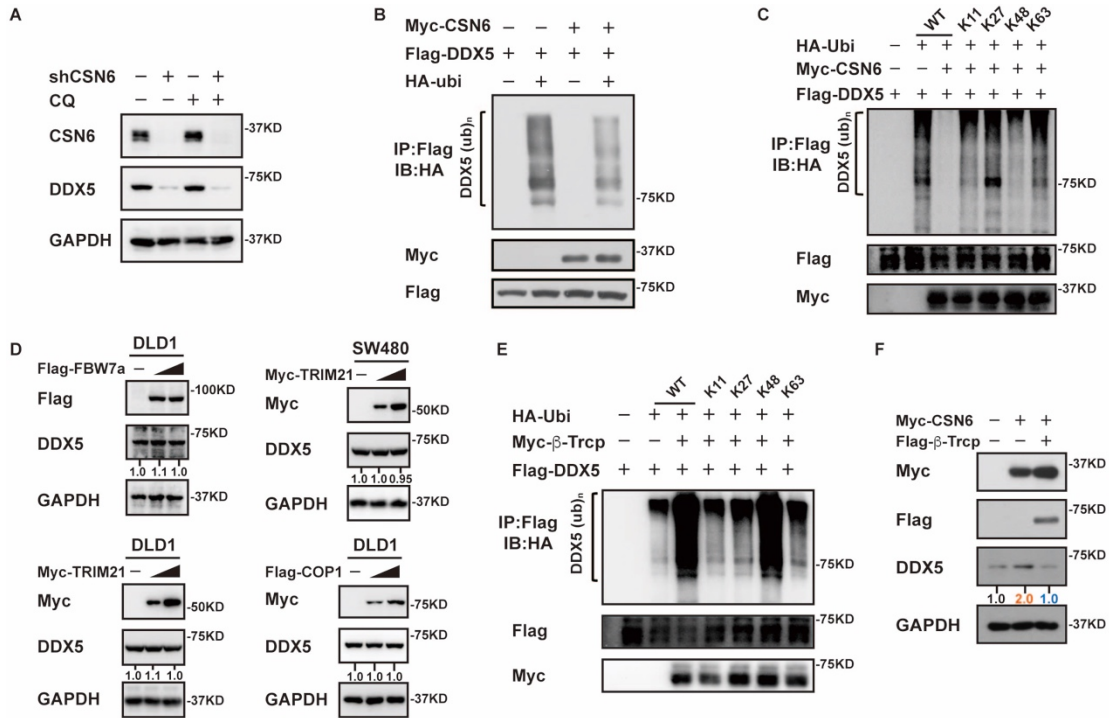
371

372

373

374

375



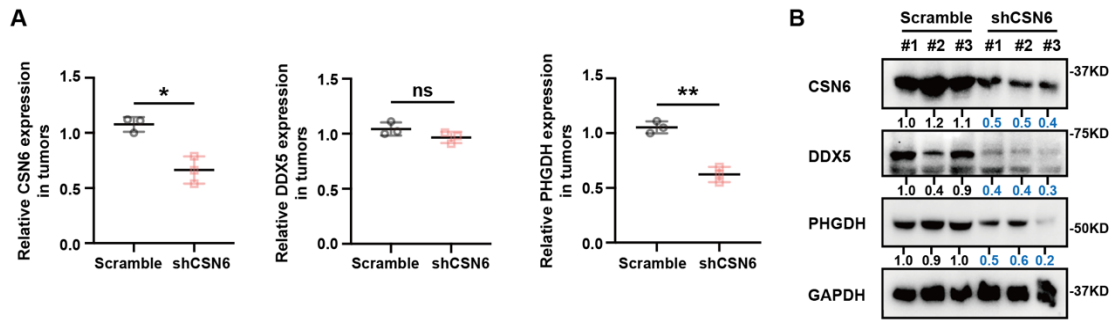
376

377 **Supplementary Fig.S8**

378 CSN6 stabilizes DDX5 protein by decreasing β -Trcp-mediated ubiquitination. **A**, Cell
 379 lysates were prepared from DLD1 cells expressing CSN6 shRNA or scrambled shRNA
 380 that had been treated with or without chloroquine (CQ) and then immunoblotted with
 381 the indicated antibodies. **B**, HCT116 cells were transfected with the indicated plasmids.
 382 MG132 was added to the cells 6 h prior to harvesting. The ubiquitinated DDX5 proteins
 383 were pulled down with anti-Flag beads and immunoblotted with the indicated
 384 antibodies. **C**, 293T cells were transfected with the indicated plasmids. MG132 was
 385 added to the cells 6 h prior to harvesting. The cell lysates were immunoprecipitated
 386 with anti-Flag beads and then immunoblotted with indicated antibody. **D**, Cells were
 387 transfected with the indicated plasmids and immunoblotted with the indicated
 388 antibodies. **E**, HEK293T cells were co-transfected with the indicated plasmids. Cells
 389 were then treated with MG132 6 h prior to harvesting. Polyubiquitinated DDX5 was
 390 immunoprecipitated with nickel beads and immunoblotted with indicated antibody. **F**,
 391 HCT116 cells were transfected with the indicated plasmids and immunoblotted with
 392 the indicated antibodies.

393

394



395

396 **Supplementary Fig.S9**

397 The expression of CSN6-DDX5-PHGDH axis in xenograft models. **A**, qPCR analysis
 398 of the indicated genes expressions in mouse DLD1 xenograft tissue samples (n = 3 per
 399 group). The data are presented as the means ± SD. *p<0.05, **p<0.01, ns: no
 400 significance, by non-parametric test. **B**, Western blot analysis of the indicated proteins
 401 in mouse DLD1 xenograft tissue samples (n = 3 per group).

402

403

404

405

406

407

408

409

410

411

412

413

414

415

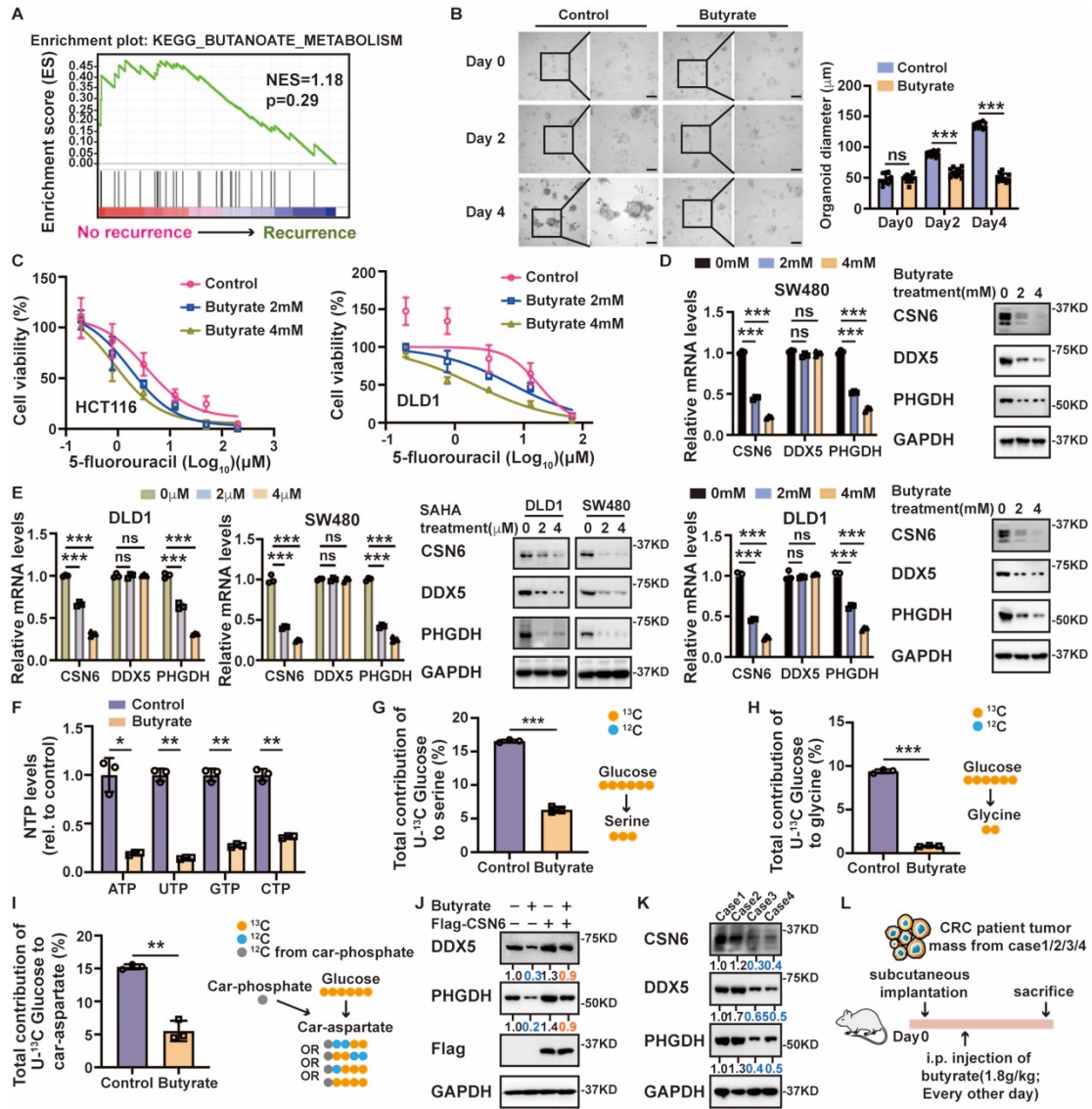
416

417

418

419

420



421

422 **Supplementary Fig.S10**

423 Butyrate may act as potential CSN6 antagonist. **A**, Gene set enrichment score and
 424 distribution of butanoate metabolism between CRC patient samples with or without
 425 recurrence. **B**, Images of organoids after 0, 2, 4 days of butyrate treatment. Scale bar:
 426 100 μ m. Quantifications of organoid diameter are presented as the means \pm SD.
 427 ***p<0.001, ns=no significance. **C**, HCT116 and DLD1 cells were treated with 5-FU
 428 at different concentrations combined with butyrate (2 mM or 4 mM) for 48 h, and the
 429 cell viability was then evaluated using the CCK8 assay. The data are presented as the
 430 means \pm SD. **D**, qRT-PCR and western blot analysis of the indicated protein levels after
 431 treatment with different concentrations of butyrate in SW480 and DLD1 cells. The data
 432 are presented as the means \pm SD. ***p<0.001, ns: no significance, by One-Way
 433 ANOVA. **E**, qRT-PCR and western blot analysis of the indicated protein levels after
 434 treatment with different concentrations of SAHA in DLD1 and SW480 cells. The data
 435 are presented as the means \pm SD. ***p<0.001, ns: no significance, by One-Way
 436 ANOVA. **F**, NTPs (ATP, GTP, UTP, CTP) levels in butyrate-treated DLD1 cells. The
 437 data are presented as the means \pm SD. *p<0.05, **p<0.01 by t-test. **G-I**, Incorporation

438 of carbon atoms from [U-¹³C] glucose into serine, glycine and car-aspartate in control
439 and butyrate-treated DLD1 cells. The data are presented as the means ± SD.**p<0.01,
440 ***p<0.001, t test. **J**, HCT116 cells were transiently transfected with Flag-CSN6 or
441 control with or without butyrate treatment, and then immunoblotted with the indicated
442 antibodies. **K**, Expression level of CSN6 in indicated patient-derived xenografts
443 (PDXs). **L**, Treatment schedule of butyrate is indicated.

444

445

446

447

448

449

450

451

452

453

454

455

456

457

458

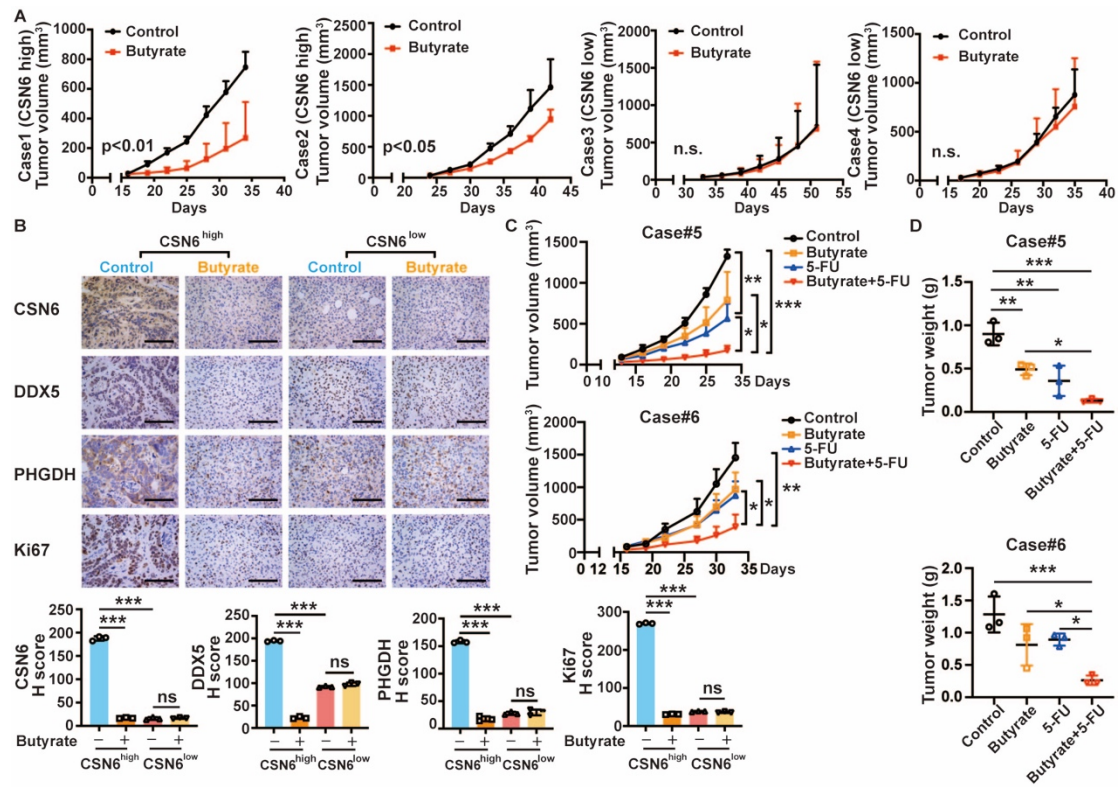
459

460

461

462

463



464

465

Supplementary Fig.S11

466

Butyrate is a CSN6 antagonist and improves the antitumor therapy efficacy. **A**, Impact of butyrate on tumor growth in mice bearing indicated PDXs. The data are presented as the means \pm SD. ns: no significance, *p<0.05, **p<0.01 by the two-way ANOVA test.

469

B, Representative IHC images and quantification of indicated proteins in CSN6 high (Case#1) or low (Case#3) PDX tumors after butyrate treatment. Scale bar: 100 μ m. For the quantification, data are presented as the means \pm SD. ***p<0.001, ns: no significance, by One-Way ANOVA.

472

C, D, Impact of butyrate and 5-FU combination on tumor growth (C) and weight (D) in mice bearing indicated PDXs. Graph represents means \pm SD. *p<0.05, **p<0.01; ***p<0.001 by the two-way ANOVA test.

475

476

477

478

479

480

481

482

483

484